Organic Thermoelectric Materials

Deutsche Ausgabe: DOI: 10.1002/ange.201604478
Internationale Ausgabe: DOI: 10.1002/anie.201604478

Bismuth Interfacial Doping of Organic Small Molecules for High Performance n-type Thermoelectric Materials

Dazhen Huang, Chao Wang, Ye Zou, Xingxing Shen, Yaping Zang, Hongguang Shen, Xike Gao, Yuanping Yi, Wei Xu, Chong-an Di, and Daoben Zhu**

Abstract: *Development of chemically doped high performance n-type organic thermoelectric (TE) materials is of vital importance for flexible power generating applications. For the first time, bismuth (Bi) n-type chemical doping of organic semiconductors is described, enabling high performance TE materials. The Bi interfacial doping of thiophene-diketopyrrolopyrrole-based quinoidal (TDPPQ) molecules endows the film with a balanced electrical conductivity of 3.3 $S\,cm^{-1}$ and a Seebeck coefficient of 585 $\mu V\,K^{-1}$. The newly developed TE material possesses a maximum power factor of 113 $\mu W\,m^{-1}\,K^{-2}$, which is at the forefront for organic small molecule-based n-type TE materials. These studies reveal that fine-tuning of the heavy metal doping of organic semiconductors opens up a new strategy for exploring high performance organic TE materials.*

With unique features in mechanical flexibility, easy processability, and low thermal conductivity, organic TE materials are promising candidates for wearable power generators.[1] The performance of an organic TE material is typically described by the figure of merit ($ZT = S^2\sigma T/\kappa$) and the power factor ($PF = S^2\sigma$), where S, σ, T, and κ are the Seebeck coefficient, electrical conductivity, absolute temperature, and thermal conductivity, respectively. Recently, great progress has been made in p-type organic/hybrid materials.[2] In comparison, only limited n-type organic/hybrid TE materials have been reported with a PF over 50 $\mu W\,m^{-1}\,K^{-2}$.[3] This uneven development makes the exploration of promising n-type organic TE materials a key issue.

Chemical doping is the strategy most widely applied for maximizing the TE performance of organic semiconductors. Schlitz et al. reported a PF of 0.6 $\mu W\,m^{-1}\,K^{-2}$, obtained by chemical doping of poly[*N*,*N*′-bis(2-octyldodecyl)-1,4,5,8-napthalenedicarboximide-2,6-diyl]-*alt*-5,5′-(2,2′-bithiophene)] (P(NDIOD-T2) with dihydro-1*H*-benzoimidazol-2-yl (*N*-DBI) derivatives.[4] Mai et al. and Segalman et al. reported a superior TE performance with self-doped conjugated polyelectrolytes and perylene diimides, which exhibited PFs of 0.84 and 1.4 $\mu W\,m^{-1}\,K^{-2}$, respectively.[5] More recently, it has been observed that effective doping of FBDPPV with *N*-DMBI can produce a high PF of 28 $\mu W\,m^{-1}\,K^{-2}$.[6] Despite these achievements, the TE performance of doped n-type organic semiconductors is not satisfactory, which is partly due to the challenges of n-type doping. Therefore, development of novel n-type doping methods for TE applications is highly desired.

Effective n-type doping of organic materials enhances TE performance by increasing carrier concentration and charge transport properties. However, many n-type semiconductors can hardly be doped with high carrier concentrations because of low electron affinity.[7] Moreover, many instances of bulk doping lead to a reduced hopping rate because of increased structural disorder.[8] Interfacial doping principally serves as a good technique for introducing a balanced carrier concentration and charge transport property to TE materials, thereby enabling a high TE performance. However, the development of efficient interfacial doping is still a challenge. Herein, we demonstrate that Bi, a heavy metal, can serve as an excellent n-type interfacial dopant for thiophene-diketopyrrolopyrrole-based quinoidal (TDPPQ) molecules. By taking advantage of high quality ultra-thin films, the Bi interfacial doping of TDPPQ yields an unexpectedly high PF of 113 $\mu W\,m^{-1}\,K^{-2}$. To the best of our knowledge, this is a record value for reported n-type small molecules. The result indicates that well-controlled metal doping of organic semiconductors can provide an excellent way toward high performance n-type TE materials.

TDPPQ is considered to be a promising TE material because of its high electron mobility and ability to facilitate superior electrical conductivity,[9] as well as its high electric field-modulated Seebeck coefficient over 600 $\mu V\,K^{-1}$ at an electrical conductivity of $> 0.1\ S\,cm^{-1}$ (Supporting Information, Figure S1).[8] However, its TE applications are limited by the efficiency of chemical doping. Although Bi is an excellent dopant for many inorganic TE materials,[10] a Bi-involved organic TE material has not been reported. Herein, Bi is explored as a dopant for TDPPQ. Figure 1 a demonstrates the mechanism of Bi interfacial doping of TDPPQ (chemical structure illustrated in Figure 1 b). The semiconductor was synthesized according to a previous report.[9]

[*] D. Huang, Dr. C. Wang, Dr. Y. Zou, X. Shen, Y. Zang, H. Shen, Prof. Y. Yi, Prof. W. Xu, Dr. C.-a. Di, Prof. D. Zhu
Department Beijing National Laboratory for Molecular Sciences
CAS Key Laboratory of Organic Solids
Institute of Chemistry, Chinese Academy of Sciences
Beijing 100190 (China)
E-mail: dicha@iccas.ac.cn
zhudb@iccas.ac.cn
D. Huang, Dr. C. Wang, X. Shen, Y. Zang, H. Shen
University of Chinese Academy of Sciences
Beijing 100049 (China)
Prof. X. Gao
Key Laboratory of Synthetic and Self-Assembly Chemistry for Organic Functional Molecules, Shanghai Institute of Organic Chemistry, CAS
Shanghai 200032 (China)
Supporting information and the ORCID identification number(s) for the author(s) of this article can be found under http://dx.doi.org/10.1002/anie.201604478.

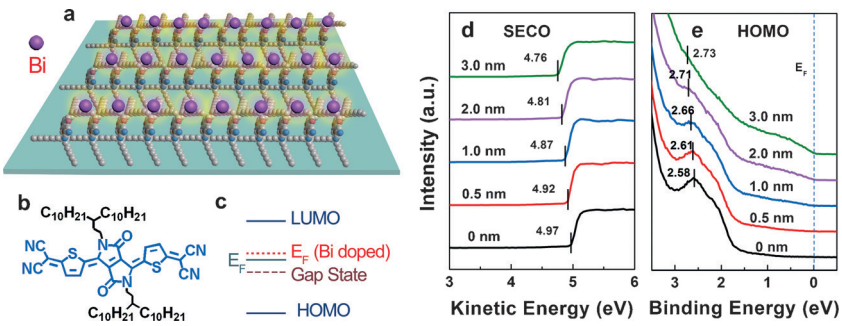

Figure 1. a) Mechanism of Bi interfacial doping of TDPPQ. b) The molecular structure of TDPPQ. c) Energy level diagram of pristine and Bi-doped TDPPQ. d) Low kinetic energy region (secondary electron cutoff) and e) low binding energy region (HOMO) of UPS during the deposition of different thicknesses of Bi on TDPPQ film.

The chemical doping of TDPPQ was firstly studied by UV/Vis absorption spectroscopy and ultraviolet photoemission spectroscopy (UPS). Since the introduction of Bi led to a red-shift of the absorption peak at 694 nm and an increase in the absorbance at 758 nm (Supporting Information, Figure S2), it is illustrated that the TDPPQ can be chemically doped by Bi. As shown in the UPS spectra (Figure 1 d), a gradual shift (ca. 0.21 eV) of the vacuum level to lower kinetic energy is observed with increasing coverage of Bi, and the work function decreases from 4.97 to 4.76 eV after deposition of 3.0 nm of Bi on TDPPQ. Similarly, after 3.0 nm of Bi coverage the characteristic feature of the HOMO peak of pristine TDPPQ (ca. 2.58 eV) gradually shifts toward higher binding energy and finally locates at approximately 2.73 eV below the Fermi level (E_F) with a possible gap state appearing at about 0.60 eV (Figure 1 e). These shifts indicate that the Fermi level of TDPPQ can shift inside the energy gap toward the lowest unoccupied molecular orbital (LUMO; Figure 1 c) because of charge transfer from Bi to TDPPQ; these observations demonstrate that n-type doping of TDPPQ by Bi has occurred. Considering a small Fermi level shift upon doping, we deduce that the TDPPQ film was lightly doped by Bi, which is consistent with the UV/Vis measurement results.

To understand the mechanism of Bi chemical doping of TDPPQ, we performed theoretical calculations on TDPPQ/Bi (Supporting Information). When a Bi atom approaches TDPPQ along the C–N triple bond of a cyano group, the doublet states of TDPPQ/Bi have the lowest total energy with weak electron transfer (0.478 e) from Bi atom to TDPPQ molecule (Supporting Information; Figures S3, S4 and S5). More interestingly, the simulated X-ray photoelectron spectroscopy (XPS) indicated that the N 1s binding energy of the Bi-linked cyano N atom becomes close to those of the DPP N atom (Figure 2). Therefore, the introduction of Bi on TDPPQ film can lead to a decrease in intensity of the low energy peak and an increase in intensity of the high energy peak of N 1s (Figure 2 b). The calculated XPS spectra are consistent with the experimental spectra (Figure 2 a), confirming that the Bi atoms interact with cyano N atoms of TDPPQ. According to these results, we propose that the appropriate work function of Bi (4.2 eV) and electron-deficient nature of TDPPQ enables electron transfer between Bi and CN, which is responsible for the Bi chemical doping of TDPPQ.

The electrical conductivity of pristine and doped TDPPQ films was measured by the four-point probe method. The pristine TDPPQ shows a low electrical conductivity $< 0.01\ S\,cm^{-1}$. When 0.5 to 3.0 nm thicknesses of Bi were deposited on the organic film, an increase in electrical conductivity was observed compared to that of a pristine film, as reflected by the obviously increased current at a fixed voltage (Supporting Information, Figures S6 and S7). To make sure that the doped TDPPQ rather than Bi contributes to the electrical conductivity of the film, we measured the electrical behavior of 3 nm of Bi on SiO_2 and glass substrates. Since no conductivity was observed, it is implied that a continuous Bi film was not formed at a thickness of ≤ 3 nm. Therefore, the increased electrical conductivity contributes from the Bi chemical doping of the TDPPQ layer.

Doping thickness is vital for calculating the electrical conductivity of doped films. We fabricated TDPPQ films with

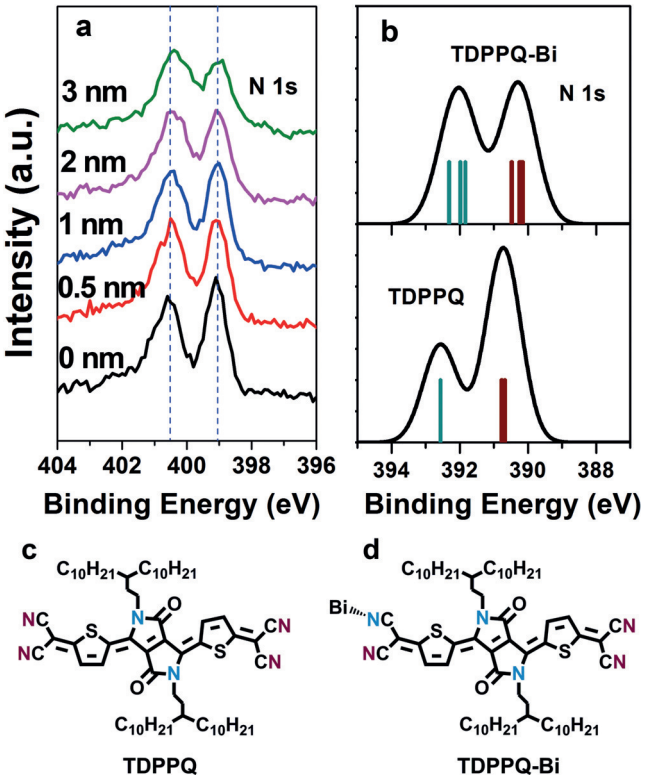

Figure 2. a) The experimental N 1s XPS spectra of pristine PDPPQ films and PDPPQ films doped with Bi. b) The calculated XPS spectra and assignment of N 1s electrons for TDPPQ and TDPPQ/Bi. The vertical lines in the XPS spectra indicate the energies of the involved N 1s orbitals and their colors correspond to the assigned atoms shown in the chemical structures in c) and d).

different thicknesses to determine the doping thickness (Supporting Information, Figure S8). It is worth noting that Bi-doped (3 nm) films exhibit improved electrical performance upon decreased thicknesses of TDPPQ (Supporting Information, Figure S9a). For instance, the resistance decreased from 4.6×10^5 to $1.1\times10^5\ \Omega$ as the TDPPQ thickness decreased from 25 to about 3 nm. Given that the thinnest film possessed the highest electrical conductivity, the chemical doping occurs at the surface of the TDPPQ film with a doping thickness approaching that of a single molecular layer. The chemical doping can be classified as interfacial doping and the electrical conductivity can be calculated with the thickness of the monolayer (3.1 nm, determined by atomic force microscopy (AFM); Figures S8a and S10). As shown in Figure S9b (Supporting Information), the electrical conductivity increased from approximately 0.7 to $>3.0\ S\,cm^{-1}$ with decreasing thickness from 25 to 3.1 nm. Of particular note is that the thinnest film exhibited a maximum conductivity of $3.2\ S\,cm^{-1}$. This electrical conductivity is among the highest values for doped n-type organic small molecules.

The surface morphology of the doped films was investigated by AFM to understand the thickness-dependent electrical behavior. Figure S10 (Supporting Information) shows AFM images of different TDPPQ films before and after Bi deposition. TDPPQ films with a thickness of about 9 nm (Supporting Information, Figure S10a and 10b) clearly exhibit a crystalline order with well-defined molecular terraces. Therefore, Bi can be deposited onto two neighboring molecular layers, as confirmed by the remaining molecular terraces and increased roughness of the films. For instance, the root mean square roughness (Rq) increased from 1.7 to 2.6 nm after deposition of 3 nm of Bi. In comparison, for the ultra-thin film with a thickness of about 3 nm (Supporting Information, Figure S10e and 10f), a nearly completely filled monolayer exhibited a much lower Rq of 0.6 nm. More importantly, chemical doping of the monolayer film occurred on a single molecular layer rather than two neighboring layers, which in turn facilitated the formation of an excellent conductive channel and improved electrical conductivity. As a result, the interfacial doping feature of TDPPQ/Bi endows the monolayer film with superior electrical performance.

To confirm that the contribution of electrical conductivity results from the doped TDPPQ layer, we measured electrical conductivity of the thin films after deposition of Bi, Au, and Al (Figure 3). In comparison with the obvious increase in electrical conductivity of Bi (1–4 nm) doped TDPPQ, slightly increased conductivity ($<0.05\ S\,cm^{-1}$) and dramatically decreased conductivity ($<10^{-5}\ S\,cm^{-1}$) were observed when 1–4 nm of Au and Al were deposited on the TDPPQ layer, respectively. However, all the films exhibited dramatically increased electrical conductivity when the metal thickness reached 4–7 nm and this value (ca. $10^5\ S\,cm^{-1}$) was maintained at a higher metal thickness of ≥8 nm. Therefore, it can be deduced that the interaction between TDPPQ and metals dominates the electrical conductivity of TDPPQ when the metal thickness is lower than 4 nm. Once the metal thickness is higher than 4 nm, the metal layer gradually dominates the charge transport, which is responsible for huge conductivities of $>10^3\ S\,cm^{-1}$. Considering that only 0.5–3 nm of Bi-dopant

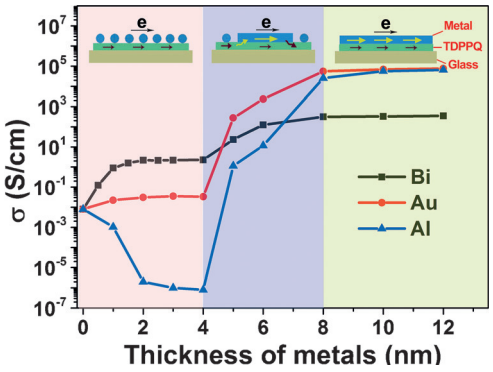

Figure 3. The electrical conductivity of ultra-thin TDPPQ films evaporated with different thicknesses of Bi, Au, and Al. The insets show the electron transfer path in the TDPPQ/metal films with varied metal thickness.

was introduced to the TDPPQ layer, it is the latter that dominates charge transport. These conclusions can be further verified by the temperature dependent electrical properties of Bi-doped films (Supporting Information, Figure S11); the doped film exhibits a similar trend compared to pristine TDPPQ film, but a different trend relative to coated Bi film.

To evaluate the TE properties of the doped TDPPQ, we examined the dopant thickness-dependent electrical conductivity and Seebeck coefficient of ultra-thin (3.1 nm) TDPPQ films. As shown in Figure 4a–c, the electrical conductivity of the TDPPQ film increased from <0.01 to $2.4\ S\,cm^{-1}$ upon deposition of 0.5–2 nm of Bi. A further increase in Bi thickness to 3 nm only resulted in a slight increase of the conductivity to $2.8\pm0.4\ S\,cm^{-1}$. In contrast, the Seebeck coefficient decreased slightly from 610 to $526\ \mu V\,K^{-1}$ after deposition of 2 nm of Bi. However, the Seebeck coefficient suffered from a dramatic decrease when 3 nm of Bi was deposited on the TDPPQ film. These results lead to an

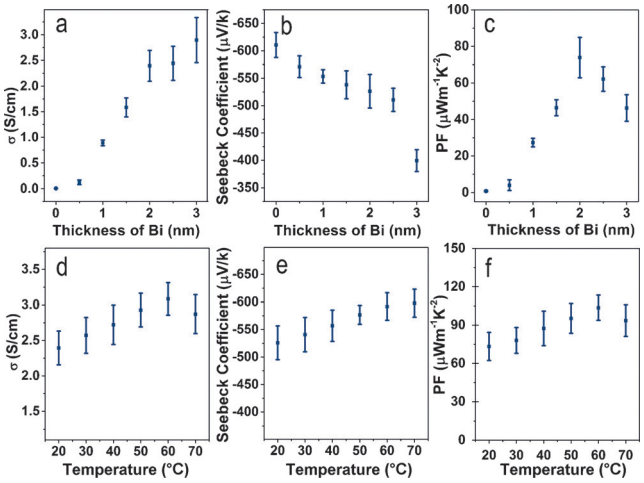

Figure 4. The thermoelectric properties of TDPPQ doped with different thicknesses of Bi. a) Electrical conductivity, b) Seebeck coefficient, c) PF as a relationship of the thickness of Bi. Temperature dependence of d) electric conductivity, e) Seebeck coefficient, and f) PF for 2 nm Bi-doped TDPPQ. Each data point in Figure 4 is an average of at least ten devices and showed good repeatability.

optimized PF of up to 62–84 $\mu W m^{-1} K^{-2}$ for 2 nm Bi-doped TDPPQ films. Additionally, the temperature dependences of the conductivity and Seebeck coefficient were investigated. As shown in Figure 4 d–f, both the electrical conductivity and Seebeck coefficient show an increasing trend as the temperature increases from room temperature to 60 °C. Therefore, it is indicated once again that the TDPPQ film dominates the charge transport properties of the doped films, which can be described by the thermally assisted hopping mechanism.[8] More importantly, the high and balanced electrical conductivity of 3.3 $S cm^{-1}$ and Seebeck coefficient of 585 $\mu V K^{-1}$ contribute to a maximum PF of up to 113 $\mu W m^{-1} K^{-2}$ at 60 °C. This performance is among the highest values reported for n-type TE materials and is even much higher than that of Cu–TCNQ,[11] a well-known metal–organic charge-transfer complex. These observations demonstrate that Bi chemical doping of organic semiconductors is an effective method for developing high performance organic TE semiconductors.

For the doped semiconductors, the carrier concentration and doping level play an important role in determining TE performance.[8] We calculated the carrier concentration by assuming that Bi interfacial chemical doping has a limited effect on mobility owing to the negligible influence of Bi on the molecular packing (Supporting Information, Figures S12 and S13).The pristine TDPPQ film possesses a low carrier concentration of $< 5 \times 10^{16}$ cm^{-3}. In contrast, a much higher carrier concentration of 1.6×10^{19} cm^{-3} is obtained with a doping level of 2.5 % after deposition of 2 nm of Bi, which dominates the enhanced electrical conductivity. This relatively low doping level is consistent with the weak chemical doping feature revealed by the UV/Vis spectra and UPS results. Given that an increase and a decrease in carrier concentration and doping level have negative effects on TE performance, it is indicated that the relatively low doping level of TDPPQ/Bi film is responsible for an outstanding PF. Unfortunately, the thermal conductivity of ultra-thin organic films can hardly be measured using conventional methods, which makes determination of the ZT problematic. However, a relatively low thermal conductivity and prominent ZT can be expected owing to the low doping level and two-dimensional-like ultra-thin film.

In conclusion, we have reported Bi interfacial doping of TDPPQ, which furnishes high performance n-type organic TE materials. Chemical doping leads to an obvious shift in the Fermi level and dramatically increased carrier concentration at the interface of TDPPQ/Bi, which in turn results in a remarkable electrical conductivity of 3.3 $S cm^{-1}$ and a Seebeck coefficient of 585 $\mu V K^{-1}$. These properties ensure a maximum PF over 110 $\mu W m^{-1} K^{-2}$. These results demonstrate that Bi is a unique and effective n-type dopant for organic semiconductors. It is worth noting that interfacially doped materials may be good candidates for the construction of Bi–organic superlattice-like materials with novel TE applications.

Acknowledgements

This research was financially supported by the Major State Basic Research Development Program (2013CB632500), the Strategic Priority Research Program of the Chinese Academy of Sciences (XDB12010000), and the National Natural Science Foundation (21422310, 61171055 and 21333011).

Keywords: chemical doping · interfacial doping · n-type materials · organic semiconductors · thermoelectrics

How to cite: *Angew. Chem. Int. Ed.* **2016**, *55*, 10672–10675
Angew. Chem. **2016**, *128*, 10830–10833

[1] a) B. T. McGrail, A. Sehirlioglu, E. Pentzer, *Angew. Chem. Int. Ed.* **2015**, *54*, 1710–1723; *Angew. Chem.* **2015**, *127*, 1730–1743; b) T. O. Poehler, H. E. Katz, *Energy Environ. Sci.* **2012**, *5*, 8110–8115; c) O. Bubnova, X. Crispin, *Energy Environ. Sci.* **2012**, *5*, 9345–9362; d) C.-K. Mai, B. Russ, S. L. Fronk, N. Hu, M. B. Chan-Park, J. J. Urban, R. A. Segalman, M. L. Chabinyc, G. C. Bazan, *Energy Environ. Sci.* **2015**, *8*, 2341–2346; e) B. Kim, H. Shin, T. Park, H. Lim, E. Kim, *Adv. Mater.* **2013**, *25*, 5483–5489; f) T. Park, C. Park, B. Kim, H. Shin, E. Kim, *Energy Environ. Sci.* **2013**, *6*, 788–792.

[2] a) O. Bubnova, Z. U. Khan, A. Malti, S. Braun, M. Fahlman, M. Berggren, X. Crispin, *Nat. Mater.* **2011**, *10*, 429–433; b) G. H. Kim, L. Shao, K. Zhang, K. P. Pipe, *Nat. Mater.* **2013**, *12*, 719–723; c) C. Cho, B. Stevens, J.-H. Hsu, R. Bureau, D. A. Hagen, O. Regev, C. Yu, J. C. Grunlan, *Adv. Mater.* **2015**, *27*, 2996–3001; d) N. Toshima, K. Oshima, H. Anno, T. Nishinaka, S. Ichikawa, A. Iwata, Y. Shiraishi, *Adv. Mater.* **2015**, *27*, 2246–2251; e) Y. Kiyota, T. Kadoya, K. Yamamoto, K. Iijima, T. Higashino, T. Kawamoto, K. Takimiya, T. Mori, *J. Am. Chem. Soc.* **2016**, *138*, 3920–3925.

[3] a) R. M. Ireland, Y. Liu, X. Guo, Y.-T. Cheng, S. Kola, W. Wang, T. Jones, R. Yang, M. L. Falk, H. E. Katz, *Adv. Sci.* **2015**, *2*, 1500015; b) H. Wang, J. H. Hsu, S. I. Yi, S. L. Kim, K. Choi, G. Yang, C. Yu, *Adv. Mater.* **2015**, *27*, 6855–6861.

[4] R. A. Schlitz, F. G. Brunetti, A. M. Glaudell, P. L. Miller, M. A. Brady, C. J. Takacs, C. J. Hawker, M. L. Chabinyc, *Adv. Mater.* **2014**, *26*, 2825–2830.

[5] a) C. K. Mai, R. A. Schlitz, G. M. Su, D. Spitzer, X. Wang, S. L. Fronk, D. G. Cahill, M. L. Chabinyc, G. C. Bazan, *J. Am. Chem. Soc.* **2014**, *136*, 13478–13481; b) B. Russ, M. J. Robb, F. G. Brunetti, P. L. Miller, E. E. Perry, S. N. Patel, V. Ho, W. B. Chang, J. J. Urban, M. L. Chabinyc, C. J. Hawker, R. A. Segalman, *Adv. Mater.* **2014**, *26*, 3473–3477.

[6] K. Shi, F. Zhang, C. A. Di, T. W. Yan, Y. Zou, X. Zhou, D. Zhu, J. Y. Wang, J. Pei, *J. Am. Chem. Soc.* **2015**, *137*, 6979–6982.

[7] C. Wan, X. Gu, F. Dang, T. Itoh, Y. Wang, H. Sasaki, M. Kondo, K. Koga, K. Yabuki, G. J. Snyder, R. Yang, K. Koumoto, *Nat. Mater.* **2015**, *14*, 622–627.

[8] F. Zhang, Y. Zang, D. Huang, C.-a. Di, X. Gao, H. Sirringhaus, D. Zhu, *Adv. Funct. Mater.* **2015**, *25*, 3004–3012.

[9] C. Wang, Y. Qin, Y. Sun, Y.-S. Guan, W. Xu, D. Zhu, *ACS Appl. Mater. Interfaces* **2015**, *7*, 15978–15987.

[10] Y. Lee, S.-H. Lo, C. Chen, H. Sun, D.-Y. Chung, T. C. Chasapis, C. Uher, V. P. Dravid, M. G. Kanatzidis, *Nat. Commun.* **2014**, *5*, 3640.

[11] Y. Sun, F. Zhang, Y. Sun, C.-a. Di, W. Xu, D. Zhu, *J. Mater. Chem. A* **2015**, *3*, 2677–2683.

Received: May 13, 2016
Revised: June 25, 2016
Published online: August 5, 2016

